Soil Control on Runoff Response to Climate Change in Regional Climate Model Simulations

BART VAN DEN HURK,* MARTIN HIRSCHI,+ CHRISTOPH SCHÄR,+ GEERT LENDERINK,* ERIK VAN MEIJGAARD,* AAD VAN ULDEN,* BURKHARDT ROCKEL,# STEFAN HAGEMANN,@ PHIL GRAHAM,& ERIK KJELLSTRÖM,& AND RICHARD JONES**

*Royal Netherlands Meteorological Institute, De Bilt, Netherlands
+Institute for Atmospheric and Climate Science ETH, Zürich, Switzerland
#GKSS Forschungszentrum, Geesthacht, Germany
@Max Planck Institute for Meteorology, Hamburg, Germany
&Rossby Centre, Swedish Meteorological and Hydrological Institute, Norrköping, Sweden
**Hadley Centre, Exeter, Devon, United Kingdom

(Manuscript received 10 June 2004, in final form 26 November 2004)

ABSTRACT

Simulations with seven regional climate models driven by a common control climate simulation of a GCM carried out for Europe in the context of the (European Union) EU-funded Prediction of Regional scenarios and Uncertainties for Defining European Climate change risks and Effects (PRUDENCE) project were analyzed with respect to land surface hydrology in the Rhine basin. In particular, the annual cycle of the terrestrial water storage was compared to analyses based on the 40-yr ECMWF Re-Analysis (ERA-40) atmospheric convergence and observed Rhine discharge data. In addition, an analysis was made of the partitioning of convergence anomalies over anomalies in runoff and storage. This analysis revealed that most models underestimate the size of the water storage and consequently overestimated the response of runoff to anomalies in net convergence. The partitioning of these anomalies over runoff and storage was indicative for the response of the simulated runoff to a projected climate change consistent with the greenhouse gas A2 Synthesis Report on Emission Scenarios (SRES). In particular, the annual cycle of runoff is affected largely by the terrestrial storage reservoir. Larger storage capacity leads to smaller changes in both wintertime and summertime monthly mean runoff. The sustained summertime evaporation resulting from larger storage reservoirs may have a noticeable impact on the summertime surface temperature projections.

1. Introduction

Climate change may be associated with a considerable change in the hydrological cycle in various regions of the world (Houghton et al. 2001). In many applications aimed at the assessment of climate-induced changes in the hydrology of large river basins, use is made of a chain of deterministic models: general circulation models (GCMs) providing global projections of present and future weather and climate, statistical or dynamical downscaling tools to enhance spatial and temporal detail of relevant meteorological forcings, hydrological models focusing on the partitioning of precipitation over evaporation, soil storage and runoff generation, and hydraulic models of the organized water transport via a river network. The downscaling step is considered to add information by explicit use of local parameters that generate meteorological variability (orography, land–sea masks, land use, and soil information, etc.; Giorgi et al. 1998; Christensen et al. 1998). Dynamical downscaling via regional climate models (RCMs) is explored widely, as to some extent it avoids assumptions of static relations between large-scale meteorological dynamics and local weather variables, as used in many statistical downscaling techniques (Murphy 2000). RCMs are maturing rapidly owing partly to coordinated activities such as the Project to Intercom-

Corresponding author address: Dr. B. van den Hurk, Royal Netherlands Meteorological Institute, P.O. Box 201, 3730 AE De Bilt, Netherlands.
E-mail: hurkvd@knmi.nl

pare Regional Climate Simulations (PIRCS; Takle et al. 1999) and international projects like the Prediction of Regional scenarios and Uncertainties for Defining European Climate change risks and Effects (PRUDENCE; Christensen et al. 2002).

Obviously, the assessment of climate change impacts on the hydrological cycle depends on the ability of the GCM and RCM systems to accurately simulate this cycle and the feedback processes acting on it. A problem often reported in GCM and RCM studies is the systematic existence of excessive continental summer drying in the simulations. Hagemann et al. (2004) considered this problem over the Danube area in more detail. Even using "perfect" boundary conditions from the 15-yr European Centre for Medium-Range Weather Forecasts (ECMWF) Re-Analysis (ERA-15), several PRUDENCE RCMs showed a pronounced continental drying. In many cases models overemphasize the positive land–atmosphere feedback that leads to a dry soil, strong evaporation stress, and reduced precipitation (see Seneviratne et al. 2002, and references therein). This poses severe problems in the interpretation of hydrological aspects of climate change in future greenhouse gas emission scenarios. If models are not successful in reproducing the regional hydrological cycle to a sufficient accuracy, their sensitivity to a changed climate forcing is likewise questionable.

A well-recognized important but sensitive component in the hydrological cycle is the land–atmosphere exchange. Like GCMs, RCMs acknowledge the role of the land surface component of the hydrological cycle by carrying a land surface parameterization (LSP) scheme that simulates the essential processes of precipitation partitioning over evaporation, storage and discharge, and the controls of both the atmospheric evaporative demand and soil water availability on the partitioning of radiant energy over sensible and latent heat fluxes. As such, they simulate the process of runoff generation and evaporation conceptually similar to hydrological models used for river discharge calculations (Giorgi et al. 1994). In some cases routing schemes are included in the RCM to directly simulate river discharge.

The land component is important since the terrestrial hydrological memory (soil water and accumulated snow amount) represents a long time scale subjective to accumulation of systematic errors and drift (Viterbo 1996; Betts et al. 1996). It is sensitive as apparently small changes to the formulation of transpiration or runoff generation may have a strong impact on the simulated hydrological cycle. Land–atmosphere feedback is shown to have a strong control on the intensity and the spatial and temporal variability of the hydrological cycle on (sub)continental spatial scales (Beljaars et al. 1996; Schär et al. 1999; Koster et al. 2000).

At least part of the problem is related to the difficulty in specifying the spatial distribution of the effective soil hydrological memory. This memory is represented by the combination of the depth of the soil water reservoir that may interact with the atmosphere via evaporation and transpiration, the temporal dynamics of precipitation, and the formulation of the dependence of evaporation and runoff on soil water content, which highly control the dynamics of the soil moisture evolution. This dynamic range is a result of choices of the shape of the hydraulic conductivity (and diffusivity) curve: near saturation, additional water storage is limited by rapid losses due to percolation, and for dry soils, additional water loss is confined by the rapid decrease of vertical water motion at low moisture contents. In addition, the shape of the canopy stress function affects the timing of the water losses by transpiration throughout the year (Lenderink et al. 2003).

The definition of effective soil hydrological memory is different from the (effective) soil hydrological capacity, which is usually indicated by a difference between field capacity and wilting point multiplied by the total soil depth. The storage range is determined by a convolution of this effective storage capacity, the temporal dynamics of precipitation, and the dependence of evaporation and runoff on soil water content. Together these variables determine the degree to which the maximum storage capacity is used throughout the annual cycle. In principle, independent information of this soil memory parameter may be derived from a combination of available information on precipitation, evaporation, and runoff. Interpretation in terms of soil hydrological capacity remains difficult as long as these regional- or continental-scale hydrological studies fail to close the water budget on an interannual time frame, but various analysis studies are reporting increasing success (Seneviratne et al. 2004; Masuda et al. 2001).

In this study the annual range of the terrestrial water storage in a range of RCMs is explored and compared to an independent estimate based on 40-yr ECMWF Re-Analysis (ERA-40) and discharge observations for the Rhine River basin (Fig. 1). The Rhine basin upstream of the Netherlands entry point near Lobith has an area of approximately 160 000 km^2. In addition, differences in response of the regional hydrological cycle to a given change in greenhouse gas concentrations are related to this terrestrial water storage capacity. The analyses in this study focus at the hydrological budget terms of the Rhine basin as a whole. Seasonal cycles are represented by processing the data in monthly averaged quantities.

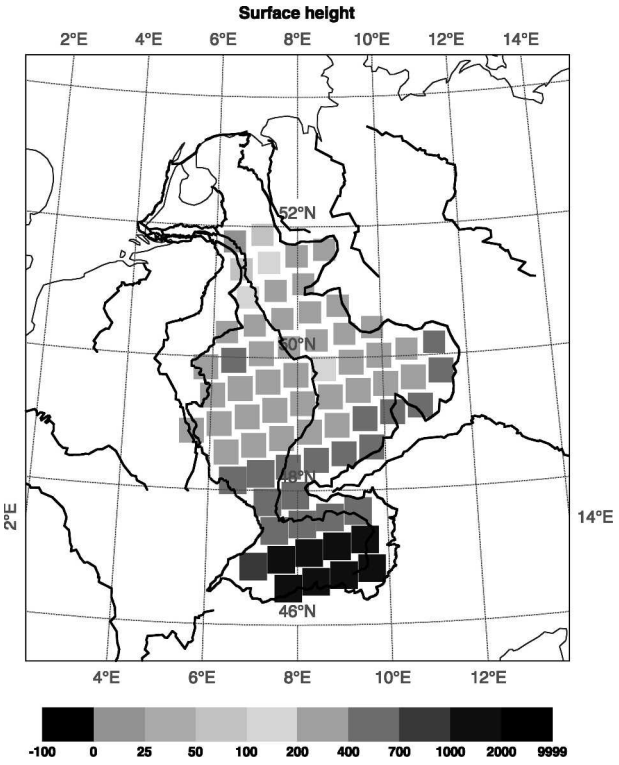

FIG. 1. Surface height in the simulation area of the Rhine catchment (surrounded by solid black line) represented at the grid of the KNMI RCM (see Table 1).

2. Datasets and models

a. The PRUDENCE simulations

In the framework of the European project PRUDENCE (see Christensen et al. 2002) a number of RCM systems were used to downscale global climate simulations from a range of GCMs and greenhouse gas emission scenarios. The RCMs differed with respect to the physical and dynamical formulations, land-use characteristics, and the grid and domain in which the models were integrated, although in all cases the models covered the major part of Europe at approximately 50-km resolution. Daily and monthly averaged output from the RCM integrations was available in a well-maintained and accessible central PRUDENCE database. From the available RCM integrations a selection was made of RCMs that (i) all simulated both a control climate (1961–90) and an A2-scenario time slice (2071–2100) derived from a specific member of the ensemble of simulations with the Hadley Centre's high-resolution atmospheric model (named HadAM3H); (ii) reported all variables that were needed to calculate the regional-scale hydrological budgets (precipitation, evaporation, runoff, snow, and soil water content); and (iii) produced a closed water balance (within 0.5% of annual precipitation) in the control simulation. From the nine RCMs meeting the first criterion, seven were used for further analysis: the Royal Netherlands Meteorological Institute (KNMI), the Danmarks Meteorologiske Institut (DMI), the Erdgenössische Technische Hochschule (ETH), the Max Planck Institute (MPI), the Swedish Meteorological and Hydrological Institute (SMHI), the GKSS Forschungszentrum (GKSS), and the Universidad Castilla la Mancha (UCM). Table 1 gives a brief overview of the specific properties of each of the RCMs.

All RCM model results are processed as time series of monthly averaged/accumulated hydrological budget terms, averaged for the whole Rhine basin. The budget terms are

$$\frac{\partial S}{\partial t} = P - E - R, \tag{1}$$

where P is total precipitation, R is total runoff, E is evaporation, and S is terrestial storage (consisting of soil and snow water content). Storage changes with time t are calculated from daily soil water and snow fields at the start of each month, whereas the flux terms in (1) are monthly averaged quantities. All terms are expressed in millimeters per day.

The depth over which S is calculated varies across the RCMs. Some models (like MPI) have a relatively deep soil of which the lower part is usually saturated and which could be considered to represent the saturated groundwater zone. Other models (like UCM) have a shallow soil that is unsaturated most of the time. In all cases, however, the water budget represented by (1) is closed. Runoff is defined as the sum of the water flux that does not infiltrate into the soil (surface runoff) plus the net flux of water leaving the soil volume via its lower boundary (the drainage component). Here $\partial S/\partial t$ is calculated over the entire soil volume between the surface and the deep boundary.

Owing to the differences in the grid orientation and resolution of the models the number of grid points used to calculate a domain-averaged quantity varies between the models (see Table 1), but this difference is considered to be of minor importance in the analysis.

The RCMs were driven by data produced by HadAM3H (Jones et al. 2001). This model has a fairly high spatial resolution of approximately 150 km and includes various changes compared to its parent coupled GCM, the Third Hadley Centre Coupled Model (HadCM3), which improves its simulation of the surface climate over many land areas (including Europe). It the context of the experiments reported here, it was used to simulate the climate of the recent past

TABLE 1. Basic description of the participating RCMs.

Acronym	No. of grid boxes in the Rhine basin	Description	References/Web sites
KNMI	69	RACMO2 model, dynamics taken from HIRLAM (version 5.0), physical parameterization from ECMWF (cycle 23R4 with increased soil storage capacity and convective triggering)	Lenderink et al. (2003)
DMI	76	HIRHAM4, with HIRLAM dynamics and the ECHAM4 physical parameterization, with adjustments in the formation of low intensity precipitation	Christensen et al. (1996)
ETH	55 (57)	CHRM, adapted from the German Weather Service high-resolution model	http://www.iac.ethz.ch/en/groups/schaer/climmod/chrm/main.html; Vidale et al. (2003)
MPI	57	REMO, based on the dynamical package of the German Weather Service model and ECHAM4 physical parameterization with various adjustments	Jacob (2001) http://www.mpimet.mpg.de/en/depts/dep1/reg/index.php
UCM	66	PROMES	Sanchez et al. (2004)
SMHI	78	Rossby Centre regional Atmosphere-Ocean model (RCAO), consisting of the atmospheric model RCA, the three-dimensional Baltic Sea ocean model RCO, and the lake model PROBE. RCA is based on the HIRLAM system with a modified land surface parameterization	Döscher et al. (2002) (RCAO) Jones et al. (2004) (RCA) Meier et al. (2003) (RCO) Ljungemyr et al. (1996) (PROBE)
GKSS	57	CLM, adapted from the German Weather Service Lokalmodell	Steppeler et al. (2003)

driven by observed sea surface temperatures (SSTs) and sea ice (SI) for the period 1960–90 and observed concentrations of greenhouse gases and emissions of sulphate aerosols. It was also used to provide a projection of the climate of 2070–2100 driven by emissions defined in the Intergovernmental Panel on Climate Change (IPCC) A2 Synthesis Report on Emission Scenarios (SRES; Nakicenovic and Swart 2000). For this experiment the sea surface forcing was derived by adding changes of SST/SI from HadCM3 driven by the same emission scenario to the observed values. Some RCM groups used the first year of the HadAM3H runs to spin up their model and reported only the last 30 yr, whereas others simply discarded the first simulation year.

b. *Analysis of the terrestrial water storage from observed large-scale quantities*

Derivation of the storage term in (1) from direct observations of soil moisture and snow amounts is not feasible when spatial scales of the order of a large river basin are considered. However, S can be estimated when the remaining terms are known. Atmospheric analysis archives have been used in the past (e.g., Trenberth and Guillemot 1995) to estimate the total atmospheric water convergence $\nabla_H Q$ in an area, which is formulated as

$$\nabla_H Q = P - E + \frac{\partial W}{\partial t}, \tag{2}$$

where Q is the total water flux (in vapor, liquid, and frozen phases) and W is the total water column at a given time. At every analysis time step, Q is calculated from the total water vapor content q and the horizontal wind speed vector $\mathbf{V}$ from

$$Q = \int_0^{p_0} q\mathbf{V}\frac{dp}{g}, \tag{3}$$

where p_0 is the surface pressure and g is the gravity acceleration. Residual terms resulting from increments in the data assimilation process, as discussed by Roads et al. (2003), are included in W. By combining Eqs. (1) and (2), $P - E$ can be eliminated. Estimation of Q from meteorological analysis fields is considered to be a better representation of the atmospheric budget than the indirect estimates of P and E from the analysis system, which are plain model forecasts only indirectly affected by the corrections that arise from the assimilation of observations. When the area of consideration matches the basin of a large river, the observed discharge from the river may be used in combination with the total convergence to infer the change of the terrestrial water storage. Seneviratne et al. (2004) demonstrated the success of this method for catchments half the size of the Rhine basin using estimates of ∇Q and $\partial W/\partial t$ derived from ERA-40. Here $\partial S/\partial t$ derived from (1) compared very well with observations from a high-resolution soil moisture, groundwater, and snow monitoring network

in Illinois. Similar networks are lacking in the Rhine basin.

Hirschi et al. (2004, manuscript submitted to *J. Hydrometeor.*, hereafter HSS) expanded on the work by Seneviratne et al. (2004) by calculating the terrestrial storage component for a number of large river basins across the world, including the Rhine. They used discharge data retrieved from the Global Runoff Data Centre (available online at http://grdc.bafg.de/servlet/is/Entry.987.Display/), which reports measured discharge amounts, not corrected for artificial reservoirs and waterworks. Kwadijk (1993) argues that water buffering in Swiss lakes has changed the mean annual cycle of the Rhine discharge noticeably, and refers to a study by Schädler (1985) to calculate the effect of lake storage on the Rhine discharge near Lobith, Netherlands. Average summertime discharge is increased by up to 9% owing to lake retention, whereas wintertime discharge is reduced by 3%–6%. The average annual cycle reported by Kwadijk (1993) has been used to correct the observed Rhine discharge data prior to calculating the terrestrial storage from the budget analysis.

Figure 2a shows a time series of the *change* of the terrestrial water storage in the Rhine basin, derived from (1) and using $\nabla Q + \partial W/\partial t$ from ERA-40 and observed Rhine discharge. As pointed out by Seneviratne et al. (2004), the large-scale budget analysis suffers from errors that are introduced from imperfect atmospheric observation systems (affecting the ERA-40 convergence estimate) and observation errors in the discharge itself. Especially in steep orographic terrain, lack of overlap of the atmospheric convergence domain and the basin producing the discharge may lead to errors in the budget calculation owing to the relatively coarse resolution of the atmospheric analysis. Also, the atmospheric assimilation system that provides estimates of the atmospheric water convergence does not conserve water, which may also affect the water balance closure. Moreover, multiyear (re)analysis time series suffer from discontinuities in the observation network, and part of the interannual variability of $\partial S/\partial t$ shown in Fig. 2a is attributed to the introduction of satellite observations since the early 1970s and insufficient spatial coverage by the rawinsonde network prior to that period. Therefore, at least part of the interdecadal variability is likely to be artificial, and is removed by subtracting a running mean with a 3-yr window. The selection of this time scale is somewhat arbitrary, but it is situated in between the seasonal time scale of soil moisture evolution and the decadal time scale at which soil moisture ranges are considered to be relatively stationary. Use of a 5-yr window instead did not have a noticeable effect on the results reported in this study. Also

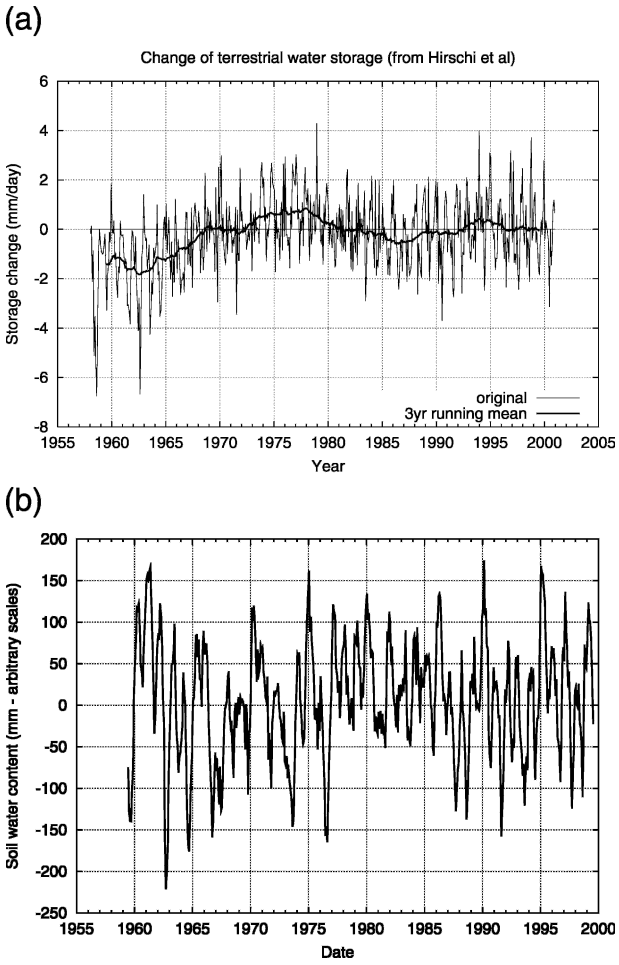

FIG. 2. (a) Time series of storage change from HSS. Shown are the original time series and a 3-yr running mean. (b) Time series of storage after filtering. Soil moisture content is expressed as total water relative to an arbitrary reference value.

using only data from 1970 onward did not significantly affect the mean annual cycles of the budget terms (Fig. 3). Subtracting a running mean can be considered as a practical means to removing apparent artificial components of the interdecadal variability while preserving as many data as possible.

The integration of the (filtered) time series in Fig. 2a results in a time series of the terrestrial storage range, shown in Fig. 2b. The position on the vertical scale is arbitrary, and defined by setting the initial soil water content at 0 mm.

An average annual cycle of the flux terms in Eq. (1) is shown in Fig. 3. In spite of a clear annual cycle of the atmospheric moisture convergence, river discharge from the Rhine shows a fairly gradual evolution. The timing of the springtime snowmelt peak varies between years, and this peak is smoothed in the 40-yr average shown in Fig. 3. The major part of the average annual

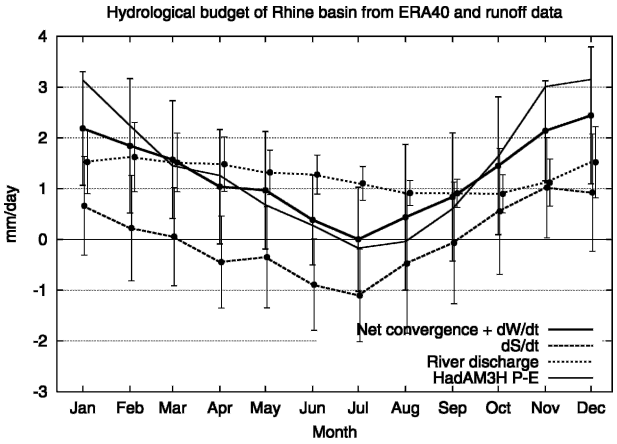

FIG. 3. Mean annual cycle of net moisture convergence plus atmospheric storage change, discharge from the Rhine, and the terrestrial storage calculated as a residual term. Error bars represent the interannual standard deviation per month. The runoff time series is corrected for reported storage in Swiss lakes, following Kwadijk (1993). Also shown is the mean annual cycle of $P - E$ from HadAM3H used to force the RCMs (thin line).

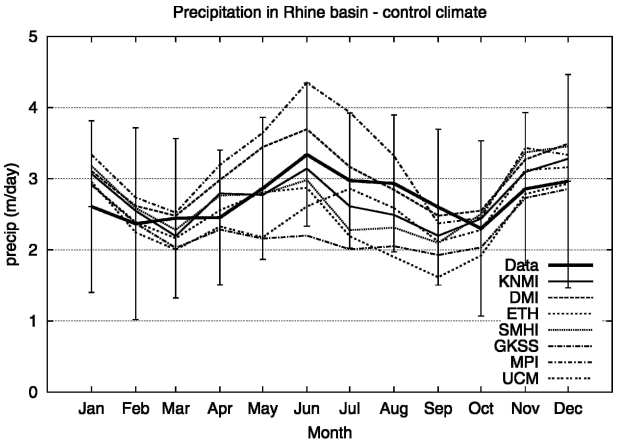

FIG. 4. Average annual cycle of precipitation over the Rhine basin from the observations (error bars representing one standard deviation of monthly means) and RCMs.

cycle in moisture convergence is buffered in the terrestrial storage reservoir (mainly the soil and groundwater reservoirs), which as a consequence displays a pronounced cycle of drying and wetting.

Also shown in Fig. 3 is the net moisture supply to the soil ($P - E$) for the same area, deduced from the 30-yr time slice of the HadAM3H control simulation representative for the 1961–90 period. Wintertime values of modeled $P - E$ are overestimated, whereas during summer a slight underestimation of net moisture supply to the Rhine basin is simulated, in particular later in the summer season. This bias is at least partly related to systematic overestimation of the frequency of blocked circulation patterns (van Ulden et al. 2004, manuscript submitted to *Climate Dyn.*).

3. Model results for present-day climate simulations

Hydrological budget terms were derived from the PRUDENCE RCM models for the same area as for which Fig. 3 is derived, the Rhine basin upstream of Lobith. Atmospheric convergence could not be calculated from (2) and (3) for most of the models (since high spatial and temporal resolution data of wind and moisture profiles were not stored), so the reported gridpoint values of $P - E$ are directly used instead. This is well justified, given the fact that all simulations conserve water mass. Here $P - E$ is compared to observed values of convergence plus atmospheric storage change in the following.

First, baseline comparisons of model results to available observations will be given for the main hydrological balance terms: precipitation, net convergence ($P - E$), runoff, and terrestrial storage. These comparisons should not be considered as direct verification since the control simulations of the RCMs were not driven by ERA-40 (as plotted in Fig. 3) but by HadAM3H, to allow evaluation of the RCM response to a change in greenhouse gas concentration. However, the intermodel variability is illustrative and can be used to highlight some basic model properties.

a. Comparison to precipitation observations

A 35-yr high density precipitation database has been compiled by the International Rhine Commission (CHR). The available precipitation database contains daily values for the period 1960–95 for 136 subbasins in the Rhine catchment area. The daily values were spatially averaged weighted by the area of each of the subbasins. Figure 4 shows a comparison between the modeled and observed average annual cycle of precipitation over the Rhine basin for each of the RCMs involved.

Most models show a considerably larger than observed range in the annual cycle, with either a peak that is too pronounced in winter or early summer precipitation or a value that is too low by the end of the summer. This variability of RCM results (driven by equal lateral boundaries) is consistent with findings of other studies (e.g., Jacob et al. 2001; Frei et al. 2003). Räisänen et al. (2004) point at a positive bias in the wintertime north–south pressure gradient over Europe in the driving GCM HadAM3H in the control climate simulation. This bias is also present in most RCM simulations, and

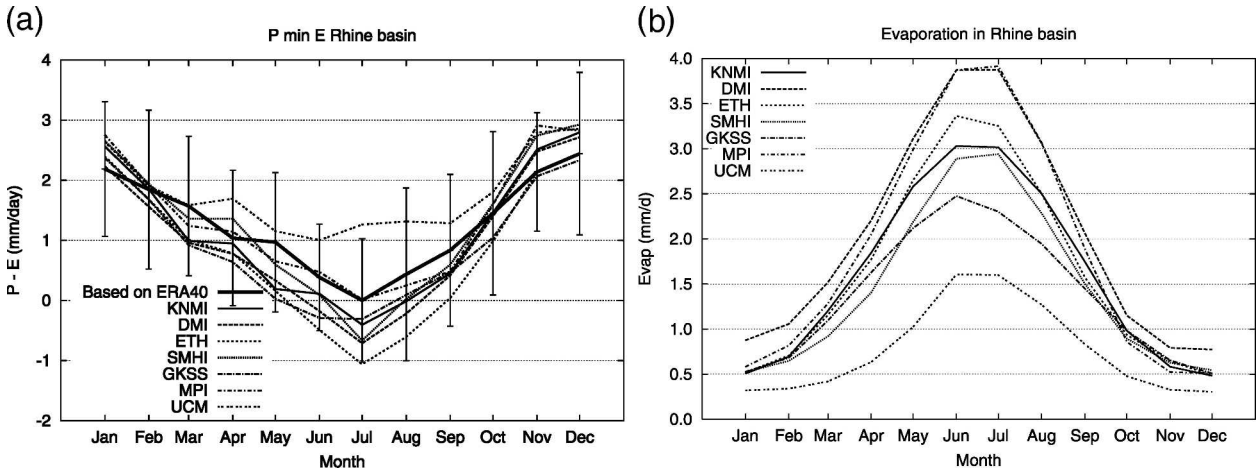

FIG. 5. Average annual cycle of (left) $P - E$ and (right) evaporation of the RCMs for the control climate simulation, and for total convergence minus atmospheric storage change derived from the estimates based on ERA-40 by HSS (error bars representing one standard deviation of monthly means).

results in an increased eastward advection of water vapor, that probably is partly responsible for the positive wintertime precipitation bias.

On the other hand, the interannual variability in the observations (shown by the error bars representing one standard deviation of the monthly means) is significant, and the average RCM results generally fall within this range.

b. Net convergence and evaporation

Large-scale observations of evaporation are not available. In principle, an estimate could be deduced by combining the ERA-40-derived estimate of $P - E$ with the CHR database shown before, but the accumulation of errors makes this estimate fairly unreliable. A direct comparison of $P - E$ between the models and the estimates derived from ERA-40 is presented here in the left panel in Fig. 5. The ERA-40-derived estimate of $P - E$ is calculated according to Eq. (2) (total convergence minus $\partial W/\partial t$), the closest possible estimate of the water flux at the land–atmosphere interface. The model-only evaporation is plotted in the right panel in Fig. 5.

The models generally have the tendency to create an annual cycle of $P - E$ that is too strong, with more convergence than observed in winter and less convergence (or more divergence) in summer. The wintertime overestimation of convergence is closely related to an overestimation of precipitation (Fig. 4). For some models the fairly good match with the observations is a consequence of compensating errors. For instance, the high summertime precipitation in MPI (Fig. 4) is effectively compensated by high evaporative loss. The lack of divergence in summertime in the UCM model is associated to fairly low evaporation amounts.

c. Discharge and runoff

The runoff generated by the RCMs is linked to the net water flux into the soil ($P - E$) and the amount of this flux that is buffered by the soil water range. The processes affecting the soil hydrological balance are mutually coupled since, in general, runoff generation depends on the soil water content. The partitioning of the net water influx over the storage change and runoff is an important property of the hydrological system, as it describes the fate of the water entering the soil: the water put into runoff is lost and cannot be re-evaporated locally, while the soil water content is a storage buffer for later evaporation or runoff generation.

Figure 6 shows the average annual cycle of the runoff generation in the Rhine basin. Also shown is the observed discharge at Lobith (the gauging station downstream of the catchment for which the modeled runoff is displayed).

Similar to the results shown in Fig. 5, the annual cycle of the modeled runoff is generally larger than the observations. The RCMs produce a fairly good wintertime runoff. Except for UCM (late) summertime runoff is too low and for some models well outside one standard deviation of the interannual variability. Also, the rate at which the runoff recovers from the summer dryness is generally much faster in the RCMs than in the observations. The ordering of models in terms of summertime runoff underestimation is roughly the same as the ordering in $P - E$ but quite different from the signature

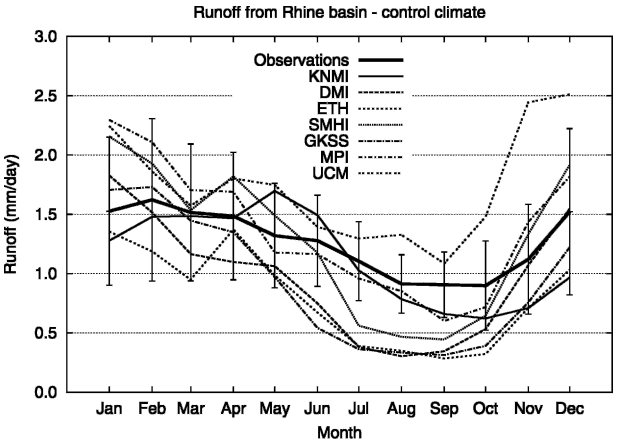

FIG. 6. Mean annual cycle of observed discharge from the Rhine basin upstream of Lobith (corrected for Swiss lake storage; error bars representing the interannual standard deviation of monthly means) and the modeled runoff from the same catchment area for the control climate simulation.

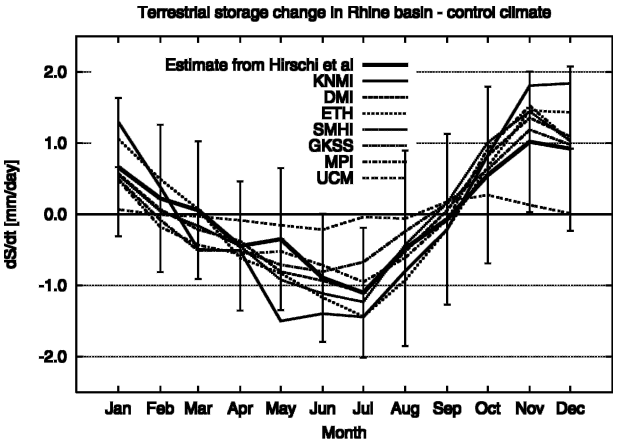

FIG. 7. Change of terrestrial storage as estimated by HSS (including the interannual standard deviation) and the RCM model output.

in the precipitation bias (Fig. 4), indicating a strong soil control (via evaporation or storage) on the runoff characteristics.

Many RCMs have systematic deficiencies in the parameterization of summertime convective precipitation over mountains. Also, the representation of glacier melt is not included. Since more than 50% of the Rhine discharge at Lobith originates from the mountainous area upstream of Basel, Netherlands, summertime runoff in the simulations is affected significantly by these deficiencies. Comparison between the observed change of the river discharge between Lobith and Basel and model generated runoff in the same catchment area indeed shows that in general the shape of the annual runoff cycle of the models is improved (results not shown). This issue will be addressed further later on.

d. Terrestrial storage

The terrestrial storage capacity in a climate model is—apart from the storage as snow—determined by the amount of water that can be stored in the soil. Many of the model parameters that have a strong influence on the actual evolution of the terrestrial water storage are difficult to specify from objective ancillary information, owing to large spatial variability, strong interaction between parameters, and the local climate dependence of the model sensitivity to the parameter values. Yet, their impact on the simulated hydrological cycle is large, and an independent evaluation of the effective (soil) storage capacity is valuable.

Figure 7 shows the storage change as estimated by HSS and the RCM model output. The interannual variability of the estimated value is considerable, and all models (except UCM) fall within this variability and show more or less a similar behavior. Except for UCM, the amplitude of the annual cycle is a bit larger than observed, in particular, in the KNMI model. However, the results are in fact surprisingly good, and in any case better than the estimate of $\partial S/\partial t$ produced by ERA-40. Over Europe, the soil water assimilation damps the annual cycle of soil water considerably (van den Hurk et al. 2004).

This "spaghetti plot" shown in Fig. 7 is not very informative on the role of the soil hydrological memory in the hydrological partitioning process, mainly because the interannual variability in the storage component is not considered. Moreover, where biases in the mean annual cycle of $P - E$, $\partial S/\partial t$, and runoff may be at least partially explained from biases in the forcing boundary conditions, the treatment of anomalously wet or dry conditions is probably a better indicator of the behavior of the individual models. Budget closure demands that anomalies in $P - E$ must be transferred into anomalies in either runoff or in the storage range. Figure 8 shows this partitioning of $P - E$ anomalies over these terms separately as deduced from the observations. The sum of discharge and storage is equal to the total $P - E$ (slope = 1.00). In this figure each symbol represents an anomaly value averaged per hydrological summer [July–August–September (JAS)] or winter [January–February–March (JFM)] season, by subtracting the average annual cycle from each monthly data point. In contrast to monthly values, anomaly correlations of summertime averages are not strongly mutually affected by the persistence of droughts or wet seasons and may be considered statistically uncorrelated.

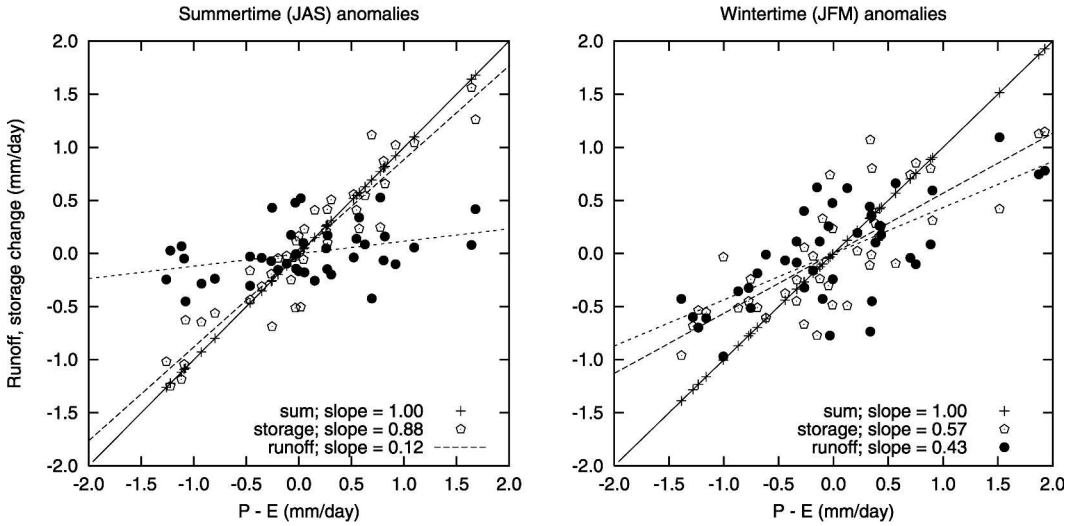

FIG. 8. Anomaly of annual (left) summertime (JAS) and (right) wintertime (JFM) terrestrial water storage and runoff as a function of the anomaly of net convergence in the Rhine basin, as derived from ERA-40 and discharge observations for all years between Jun 1960 and Jul 1999. Also shown is the sum of storage and runoff, and the linear slope values of the least squares fits.

Given the fairly small average annual cycle in the discharge observations (Fig. 4), it is not surprising that anomalous water supplies to the basin area are primarily buffered in the soil and snow components, and that only ~13% of the anomalies are transferred as discharge within the same season.

In summertime the storage range has on average a large uptake capacity, and anomalies in convergence are rapidly absorbed in the soil. In wintertime, this buffer capacity is less and a stronger preference for discharge is displayed. However, the discharge response is still the smaller component in the partitioning of $P - E$ anomalies.

A similar analysis was carried out for the area downstream of Basel, where complex precipitation or glacier processes in mountainous areas are less significant. The correspondence between annual total $P - E$ derived from ERA-40 and runoff was indeed improved (thus, the bias in the terrestrial storage reservoir shown in Fig. 2a was smaller). The correlation between $P - E$ anomalies and runoff was reduced from 13% to 4%, consistent with the elimination of the high Alpine mountain area with small storage capacity from the domain. In winter the correlation reduced from 42% to 30%.

Do the RCMs explored here reproduce this basin response under present-day climate conditions? Figure 9 shows similar plots as in Fig. 8 from two participating models as an example, and Fig. 10 summarizes the wintertime and summertime regression slopes of anomaly partitioning components. An uncertainty estimate of these regression slopes is calculated using the bootstrapping method, by calculating the standard deviation of the regression coefficient of 10 000 sets of 30 pairs.

The comparison between the anomaly partitioning in the observed data and the RCMs reveals three groups of models: the KNMI model with a higher-than-observed portion of the anomalies put in the storage and less in the runoff, the UCM model that has a very small storage capacity and consequently a strong runoff response to convergence anomalies, and the remaining models that are in between these two extremes but have a lower-than-observed contribution of the storage term. Except for UCM, the relative differences between all models and observed records are preserved when the analysis is carried out for separate season periods. During the summer months, the KNMI model reproduces about the right partitioning when compared to the Hirschi analysis, but in winter the significance of the storage range is overestimated. All other models have a correlation between runoff and $P - E$ that is too strong both in summer and in winter. The difference in behavior between the KNMI model on one hand and ETH as example for the others is well discerned in Fig. 9. The impact of this difference in correlations on the sensitivity of the modeled regional hydrological cycle to climate change is explored in the next section.

The analysis was also carried out for the domain downstream Basel, to eliminate the possible effects of deficiencies in precipitation or glacier melt in the high mountain area. For all models, the summertime correlation between $P - E$ anomalies and runoff decreased

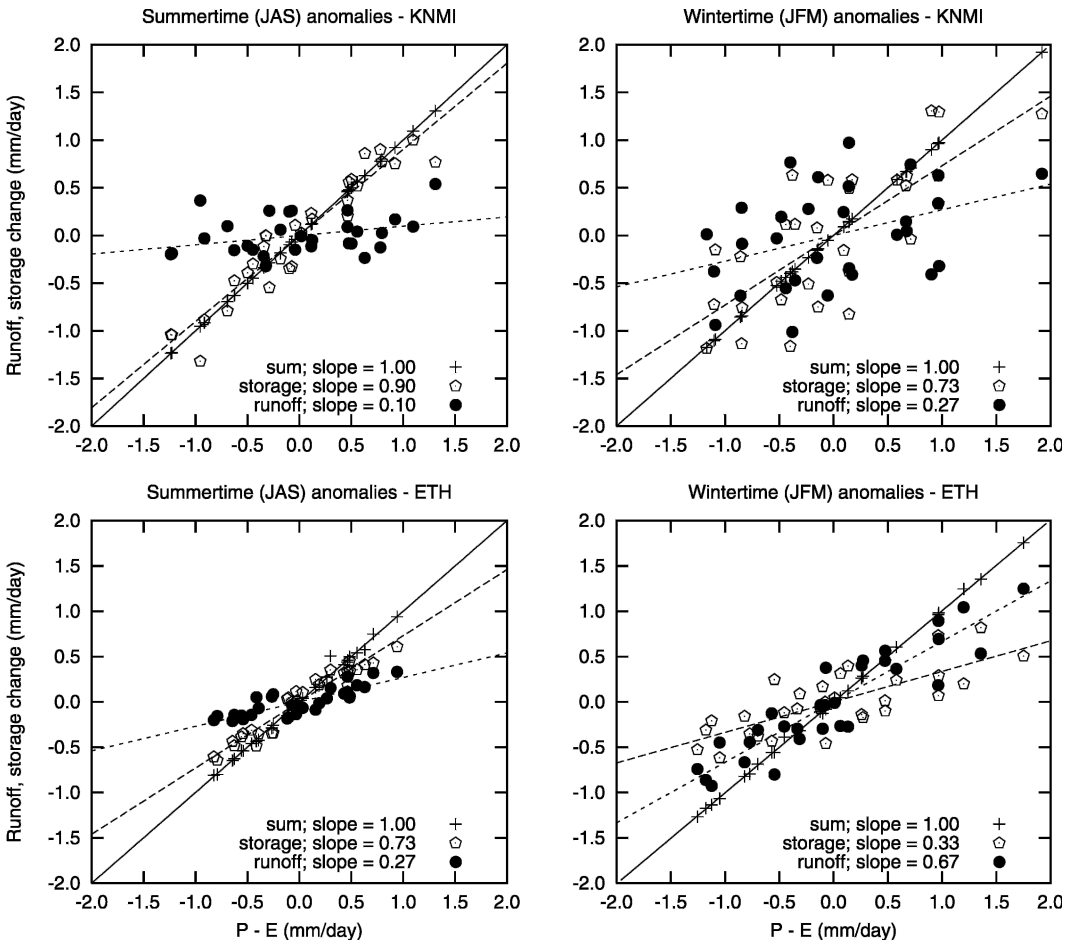

FIG. 9. Same as in Fig. 8, but for model simulations from two RCM models: (top) KNMI and (bottom) ETH for (left) summer (JAS) and (right) winter (JFM) months.

by 5%–10%, similar to the reduction of the equivalent correlation in Hirschi's analysis. The wintertime correlation coefficients changed approximately 5%, but not into the same direction for all models.

4. Modeled response to a climate change scenario

a. Response of runoff to climate change

All participating models also performed a 30-yr simulation (2071–2100) driven by the HadAM3H model in which the A2 greenhouse gas emission scenario was imposed. Among other effects, the selected scenario leads to increased winter precipitation and decreased summer precipitation in the Rhine basin (Fig. 11). The range of simulated changes in precipitation across the models is about 0.5 mm day^{-1}, which is considerably less than the >2 mm day^{-1} range displayed in the simulated present-day precipitation climate (Fig. 4). The range in simulated precipitation rates in each of the control and A2 scenario experiments is significantly larger than the range of the simulated responses to the A2 greenhouse gas scenario.

Intermodel differences in evaporation are most pronounced in summer, where parameterized soil processes control the water loss to the atmosphere (Fig. 11c). The KNMI model with the relatively large storage range (Fig. 11d) can sustain a longer period where $E > P$, even when both E increases and P decreases. A high evaporation rate is also sustained in the simulation by UCM, which compensates the low evaporation in the control simulation (Fig. 5) under conditions of higher air temperatures. In the UCM simulation the water is not provided from a terrestrial reservoir (which has a very small buffer capacity) but from a smaller-than-average precipitation reduction and larger-than-average runoff reduction (Figs. 11b,e, respectively). A rapid response owing to a limited soil water range is

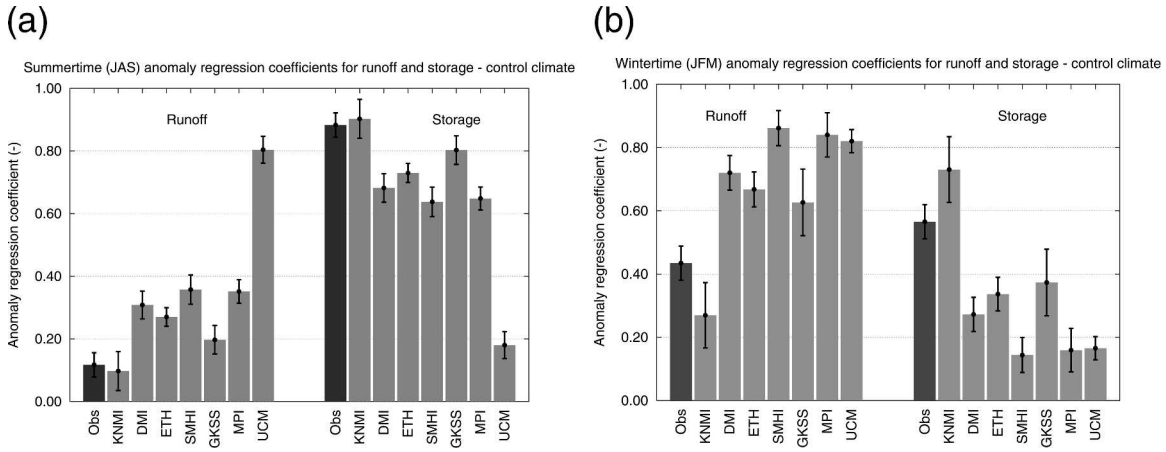

FIG. 10. Slope of monthly runoff and storage anomaly as a function of anomaly in $P - E$ for the participating RCMs for (left) summertime and (right) wintertime. "Obs" refers to the analysis by HSS.

particularly evident in the simulation by SMHI, where the evaporation response to the A2 scenario rapidly changes sign between June and August.

The translation of the precipitation change into the runoff response is highly variable, in particular in the winter season. In general, the seasonal variation of runoff increases in the A2 scenario (more runoff in winter, less in summer), but the magnitude of this increase is much smaller in the KNMI model than in the others.

Figure 12 shows a summary of the change in the seasonal cycle of runoff in relation to the depth of the soil water range in the models. The change in seasonal cycle of runoff is indicated by plotting the fraction of total runoff that occurs in the summer months (JAS; left panel): higher values of this fraction indicate smaller differences between summertime and annual mean runoff. When runoff is identical in all months, the fraction is 0.25 (3 out of 12 months) per definition. The depth of the soil water range, denoted by D hereafter, is defined as the difference between the 95% and 5% percentiles in the 30-yr time series of monthly stored water. As indicated before, this definition is different from the (effective) soil storage capacity, which is usually indicated by a difference between model-dependent field capacity and wilting point multiplied by the total soil depth. Similar to the high-pass filtering in the observed time series (Fig. 2a), a 3-yr running mean was subtracted from the soil water time series prior to calculating the storage range to remove slow trends in the budget calculation. The interannual variability is estimated by calculating the standard deviation of the yearly difference between maximum and minimum amount of stored water. The value of the "observed" soil water range, also indicated in Fig. 12, must be interpreted with some caution, since it is calculated as a residual term of the water budget equation.

Consistent with Fig. 11, Fig. 12 shows that in all models the fraction of annual runoff generated during summer decreases in all models when changing from the control to the A2 simulation. Simultaneously, the winter fraction increases. Also shown is an increase of the annual storage range in all models when an A2 scenario is imposed. Wetter winters and dryer summers both expand the range of D: wetter winters partially due to increased maximum snow depth and higher soil saturation degrees when rainfall and snowmelt rapidly recharge the drained soil water, and dryer summers due to increased atmospheric evaporative demands that is attenuated by bringing the level where soil water stress inhibits evaporation to lower moisture levels.

However, in contrast to Fig. 11, the display in Fig. 12 enables us to relate the degree of the change of the runoff seasonality to the model-specific value of D. Models with a small terrestrial water buffer (extreme case: UCM; see also Fig. 7) have a smaller change of D in case of an A2 scenario, and a relatively strong increase of the runoff seasonality. Models with larger soil water buffers (extreme case: KNMI) show a smaller response of the runoff seasonality to a change in $P - E$, as shown clearly in Fig. 12. The relative summertime runoff for the area downstream of Basel is approximately 5% lower than the results plotted in Fig. 12, and in winter it is 5% higher, but the grouping of models is not clearly affected by the choice of the catchment domain (results not shown).

The response of runoff anomalies to anomalies in net convergence, as displayed in Fig. 10 for present-day climate conditions, may be indicative of the way the models respond to a change in the greenhouse gas sce-

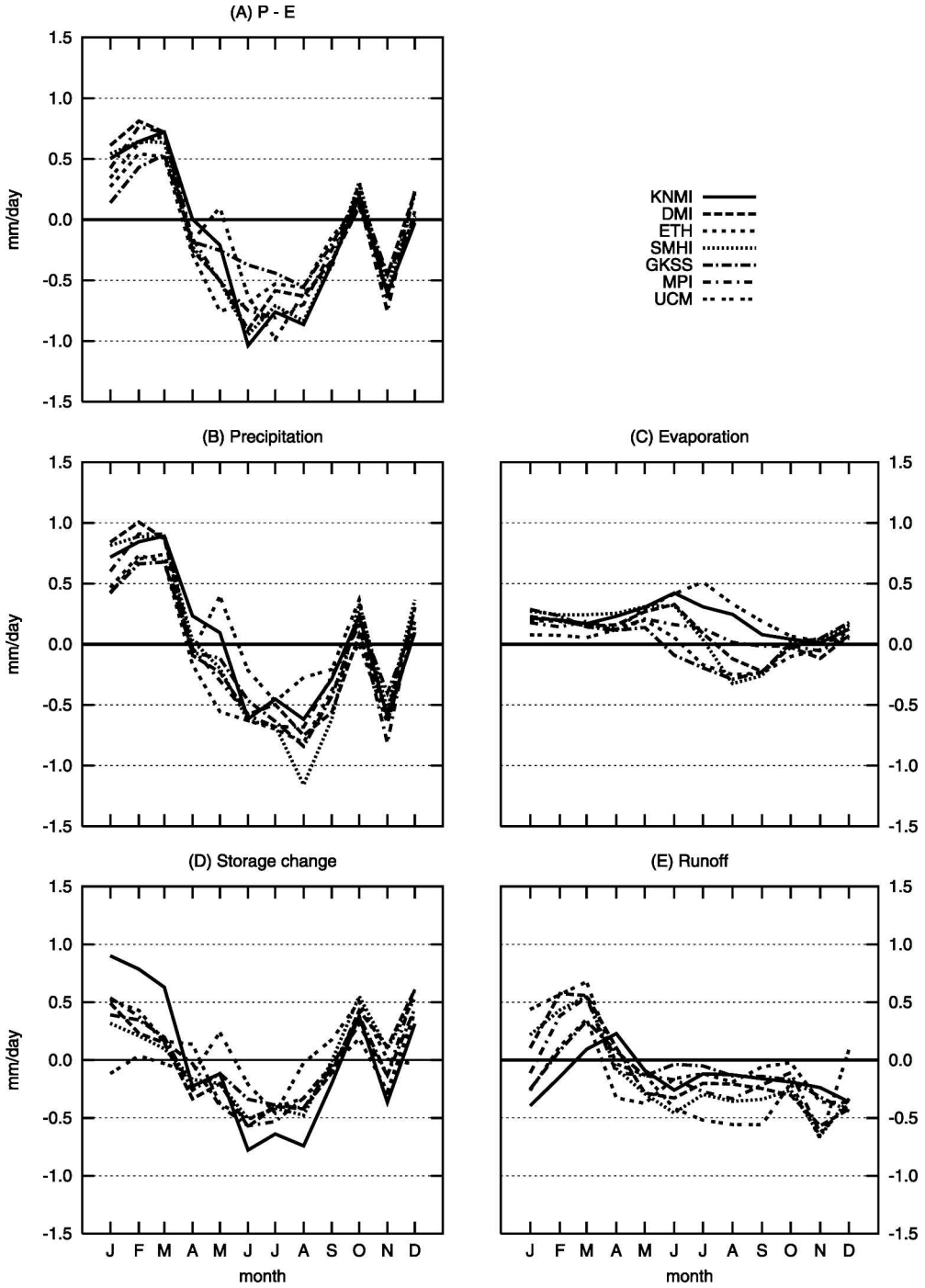

FIG. 11. Difference in average annual cycle of modeled (a) $P - E$, (b) precipitation, (c) evaporation, (d) storage change, and (e) runoff in the Rhine basin between A2 and control simulations.

nario. To first order, the transition to an A2 scenario generates a different net convergence, which can be considered as an anomaly compared to the present-day climate reference situation. Figure 13 displays a similar plot as in Figs. 8 and 9, but now showing the multiyear mean values of R and $P - E$ for each 30-yr simulation, grouped per model. For reference, also the slope of the response of runoff anomalies to anomalies in net convergence, as displayed in Fig. 10 for the control climate simulations, is displayed. For the summer period, the slopes shown in Fig. 10 are very similar for the A2 scenario simulations for nearly all models (not shown).

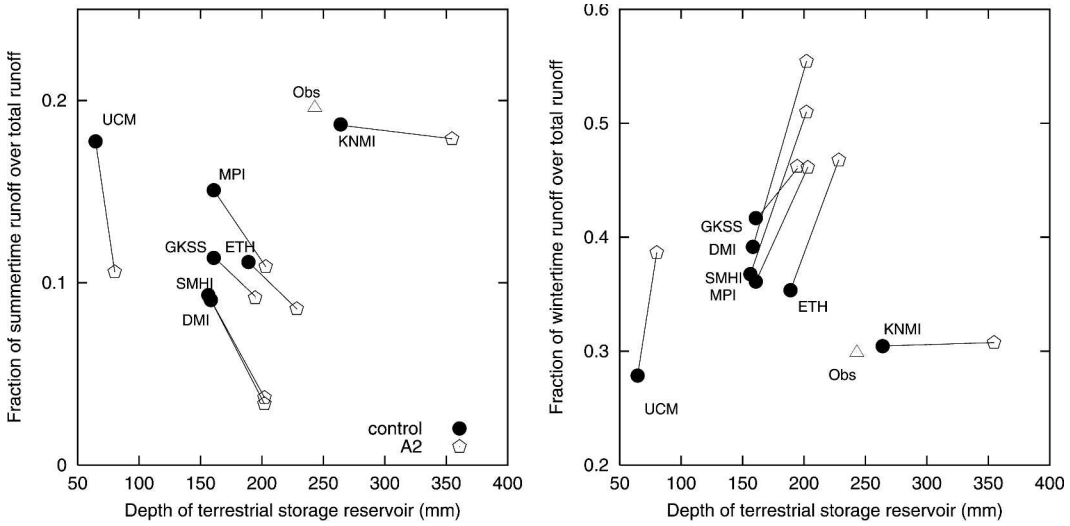

FIG. 12. (left) Summertime (JAS) and (right) wintertime (JFM) runoff divided by annual total runoff vs depth of terrestrial storage reservoir. Each symbol represents the multiyear average of a single RCM. Shown are simulations for control and A2 climate scenarios, and each RCM pair of scenario calculations is connected with lines. Observations are shown as well.

This is due to the fairly straightforward coupling between net water supply ($P - E$) to the soil and partitioning this supply over storage and runoff.

The response of the runoff anomaly to $P - E$ anomalies in the control simulation in each model is indicative for the response of the model to a change in greenhouse gas scenario. Although a solid correlation between these two responses is not consistently present in Fig. 13, a small anomaly response can clearly be associated with a smaller greenhouse gas response. Thus, the anomaly of $P - E$ translates similarly into a summertime runoff anomaly, as does the multiyear averaged runoff respond to multiyear averaged net convergence between two climate change scenarios. This implies that the interannual variability of $P - E$ versus runoff, derived from the observations (Figs. 8 and 10), may be used as a proxy of the response of mean runoff to climate change. The climate response is gradually oriented steeper when models are situated in the bottom right portions of the plot. Again, the KNMI and UCM models are relative outliers in the transition of induced changes of $P - E$ into runoff changes: KNMI putting smaller portions of $P - E$ anomalies into runoff (resulting in a small runoff response to climate change shown in Fig. 10), whereas UCM rapidly transfers $P - E$ anomalies into runoff. All other models group around the same slope of $\Delta R/\Delta(P - E)$, although the absolute values of the runoff in the control simulation vary widely across models.

In wintertime (Fig. 13, bottom panel) $P - E$ increases in all RCM simulations, but runoff averaged over JFM decreases (slightly) for the KNMI model, in contrast with the general increase of wintertime runoff in response to climate change in the other models. However, the deduction of the RCM response to a change in $P - E$ from the interannual variability in simulations of either climate forcing is less straightforward than in winter. In general, the simulated runoff in wintertime is much less correlated to the supply of water to soil alone, but is highly dependent on the accumulation and melt of snow, existence of frozen ground, and direct response to precipitation in case of saturated soils. However, from Fig. 13 it can be deduced that the depth of the annual cycle of the terrestrial storage is larger than average in the KNMI model, and this buffer capacity helps keeping the runoff response to increases in wintertime precipitation relatively low (see also Fig. 12, right panel).

b. *Response of summertime temperature*

Simulated temperature changes under climate change conditions are dependent on many interacting processes embedded in the RCM codes. Summertime temperature responses over land are considered to be partially sensitive to the representation of the hydrological cycle (e.g., Schär et al. 2004). Under present-day climate conditions, many RCMs suffer from an excessive continental drying, which is related to a chain of processes linking evaporation to stored soil water, local precipitation to local evaporation, interaction between the hydrological cycle and large-scale dynamics, and

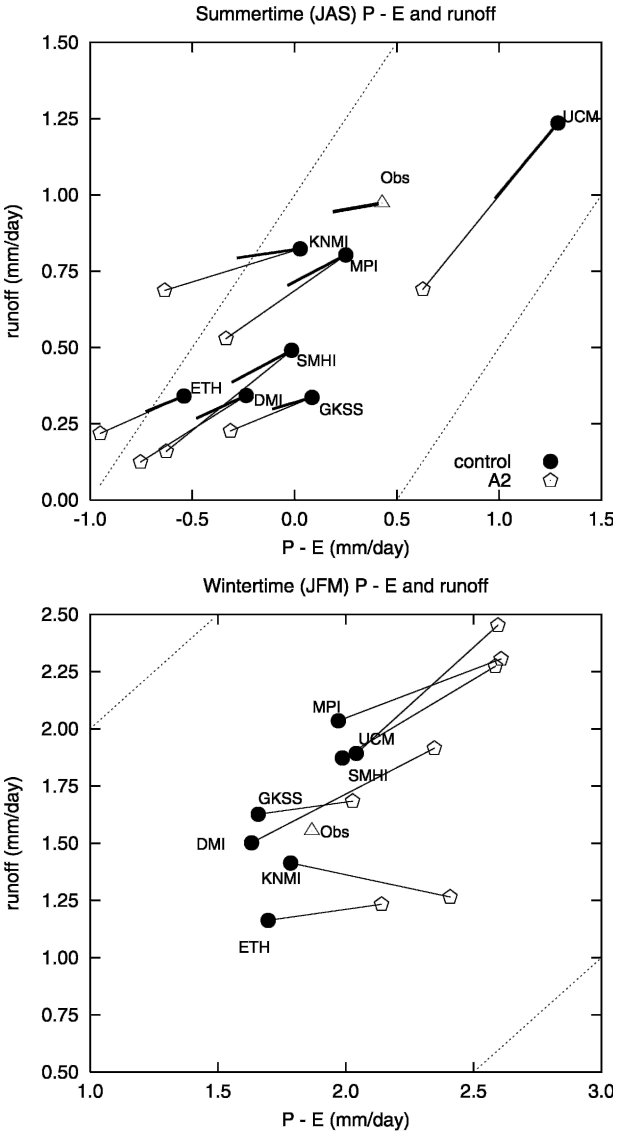

FIG. 13. (top) Summertime (JAS) and (bottom) wintertime (JFM) total runoff vs $P - E$. Shown are seasonally averaged fluxes with error bars representing the interannual standard deviation. Each symbol represents a single RCM for control (red) and A2 (green) simulations. Control–A2 pairs of each RCM are indicated by the blue connecting lines. The heavy lines originating from each symbol in the top figure represents the best-fit linear slope of runoff vs $(P - E)$. In the winter plot (bottom) these lines are not plotted. Also, observations are shown (in black). Thin dashed lines indicate a 100% transfer of $P - E$ anomalies into runoff anomalies.

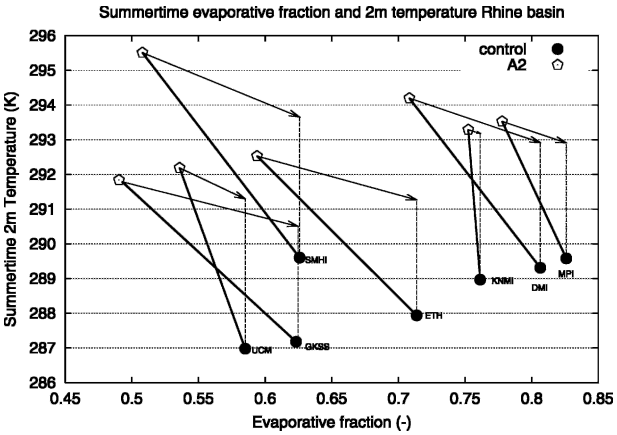

FIG. 14. Average summertime 2-m temperature as function of the evaporative fraction for both the control and A2 scenario model simulations. Arrows departing from the A2 symbols represent the virtual reduction of summertime temperature if the evaporative fraction remained unchanged between the control and A2 scenario simulations. The slopes of the arrows are derived from the interannual variability of $\partial T/\partial\Lambda$ in the simulations.

the dependence of the precipitation efficiency on the thermodynamic structure of the atmosphere (Schär et al. 1999). Clearly, the depth of the soil water range plays an important role in the annual cycle of evaporation and its response to climate change (cf. Fig. 11), and it is worthwhile to explore whether this effect on evaporation has a clear impact on the response of the near-surface temperature to climate change.

High values of net radiation and low values of evaporation are generally both associated with high near-surface temperatures. The relation between evaporation and temperature is therefore more ambivalent than the relation between evaporative fraction Λ (latent heat flux divided by net radiation, ignoring soil heat flux) and temperature. Here T and Λ are negatively correlated, with values of $\partial T/\partial\Lambda$ ranging between -4 and -20 K for the model simulations.

Figure 14 shows the multiyear mean summertime 2-m temperature and evaporative fraction for all 30-yr simulations, again grouped per RCM. In general, the calculated summertime evaporative fraction is reduced by approximately 6%–8% when changing the climate scenario from control to A2, and simultaneously the summertime temperature increases between 4 and 6 K. For each of the models, the average value of $\partial T/\partial\Lambda$ is calculated using both the control and A2 30-yr simulations. This slope is used to estimate the contribution of the change of Λ to the change of T, naively assuming that the temperature response is a linear superposition of a hydrologically controlled component and an "autonomous" increase due to remaining processes (radiative absorption, change of circulation statistics, etc.). Suppose that all models keep the summertime evaporative fraction in the A2 simulations similar to the control simulations, simple extrapolation of $\partial T/\partial\Lambda$ results in a reduction of the summertime temperature increase with 0 (KNMI) to up to nearly 2 K (SMHI).

5. Discussion and conclusions

The PRUDENCE RCM simulations have been analyzed in terms of the soil hydrological budget components in the area encompassing the Rhine basin. Derivations from major terms in the hydrological budget equation were taken from ERA-40, precipitation observations from CHR, and discharge observations for the Rhine, and these data served as background material.

Not surprisingly, the RCM models involved show a great variability in all simulated terms. The seasonality in precipitation, evaporation, and net atmospheric convergence ($P - E$) are generally captured (although systematic biases in the driving GCM are obviously not removed), but the magnitude of the seasonal fluxes deviates from the observed or derived quantities. The largest relative errors occur with the runoff generation, which is the smallest term in the balance equation. Part of the overestimation of the annual cycle of runoff is related to systematic deficiencies in hydrological processes in mountainous areas.

In general, most models simulate a correlation that is too strong between anomalies in $P - E$ and runoff. Anomalous moisture fluxes into the soil are not buffered enough by the terrestrial water stores (soil water and snow), and the seasonality of simulated runoff is without exception larger than observed. Runoff schemes in RCMs are not necessarily designed for accurate discharge calculation, but they do respond to general water balance tendencies. Errors in simulated runoff of the sizes found may be directly linked to the errors of the overall water budget in applications where RCMs are one- or two-way coupled to more sophisticated hydrological/hydraulical model systems. Drastic inconsistencies in the fluxes "seen" by the hydrological models and by the RCMs are the result. Given the importance of the atmospheric feedback to land surface evaporation, this inconsistency makes application of these coupled systems in climate change scenario analysis an area of further development.

Also, the climate change response in the RCMs themselves shows a wide range. In general, schemes with larger buffering capacities show smaller responses of runoff to changes in net convergence. The relation between summertime runoff and $P - E$ as derived from the interannual variability in the control simulations match fairly well the average response to a changing climate. Therefore the interannual variability in the observations, and in particular the anomaly correlation between $P - E$ and runoff anomalies, are an important verification tool for the RCMs. The comparison made here favors models with larger terrestrial storage capacities.

Wintertime runoff is less directly responding to $P - E$ anomalies, but also here smallest responses to precipitation regime changes occur with larger terrestrial storage, even when the precipitation regime changes quite drastically. In addition, the interannual variability of wintertime runoff—an important quantity to estimate future risks of extreme floodings—is smaller for strongly buffered schemes.

The relation between soil hydrology and near-surface temperature is less straightforward than the relation with runoff. In the simulations, the interannual variability of summertime near-surface temperature response is well anticorrelated to the interannual variability of the evaporative fraction. Although this is not necessarily a causal relation, the crude statistics show that eliminating climate change effects on summertime evaporation by increasing the terrestrial water buffer could mitigate the temperature response by 0 to 2 K. Repeated simulations with increased effective buffer capacity in each of the models is necessary to confirm this rather naive assumption.

Acknowledgments. The Hydrological Rhine Committee (CHR) is acknowledged for making the precipitation database available. The PRUDENCE team supervised by J. H. Christensen and O. B. Christensen has been an inspiring discussion platform and is acknowledged for making various model simulations available. Fruitful discussions with Eric Wood, Adri Buishand, Hendrik Buiteveld, and Pedro Viterbo helped to improve the manuscript. Manuel Castro is acknowledged for making the UCM model results available.

REFERENCES

Beljaars, A. C. M., P. Viterbo, M. J. Miller, and A. K. Betts, 1996: The anomalous rainfall over the United States during July 1993: Sensitivity to land surface parameterization and soil moisture anomalies. *Mon. Wea. Rev.,* **124,** 362–383.

Betts, A. K., J. H. Ball, A. C. M. Beljaars, M. J. Miller, and P. Viterbo, 1996: The land surface–atmosphere interaction: A review based on observational and global modeling perspectives. *J. Geophys. Res.,* **101,** 7209–7225.

Christensen, J. H., O. B. Christensen, P. Lopez, E. van Meijgaard, and M. Botzet, 1996: The HIRHAM4 regional atmospheric climate model. Scientific Rep. 96-4, Danish Meteorological Institute, Copenhagen, Denmark, 51 pp.

——, T. Carter, and F. Giorgi, 2002: PRUDENCE employs new methods to assess European climate change. *Eos, Trans. Amer. Geophys. Union,* **82,** 147.

Christensen, O. B., J. H. Christensen, B. Machenauer, and M. Botzet, 1998: Very high resolution regional climate simulations over Scandinavia—Present climate. *J. Climate,* **11,** 3204–3229.

Döscher, R., U. Willén, C. Jones, A. Rutgersson, H. E. M. Meier, U. Hansson, and L. P. Graham, 2002: The development of the coupled regional ocean–atmosphere model RCAO. *Boreal Environ. Res.,* **7,** 183–192.

Frei, C., J. H. Christensen, M. Déqué, D. Jacob, R. G. Jones, and P. L. Vidale, 2003: Daily precipitation statistics in regional climate models: Evaluation and intercomparison for the European Alps. *J. Geophys. Res.,* **108,** 4124, doi:10.1029/2002JD002287.

Giorgi, F., S. W. Hostetler, and C. Shields Brodeur, 1994: Analysis of the surface hydrology in a regional climate model. *Quart. J. Roy. Meteor. Soc.,* **120,** 161–183.

——, L. O. Mearns, C. Shields, and L. McDaniel, 1998: Regional nested model simulations of present day and $2 \times CO_2$ climate over the central plains of the US. *Climate Change,* **40,** 457–493.

Hagemann, S., B. Machenauer, R. Jones, O. B. Christensen, M. Deque, D. Jacob, and P. L. Vidale, 2004: Evaluation of water and energy budgets in regional climate models applied over Europe. *Climate Dyn.,* **23,** 547–567.

Houghton, J. T., Y. Ding, D. J. Griggs, M. Noguer, P. J. van der Linden, X. Dai, K. Maskell, and C. A. Johnson, Eds., 2001: *Climate Change 2001: The Scientific Basis*. Cambridge University Press, 881 pp.

Jacob, D., 2001: A note to the simulation of the annual and interannual variability of the water budget over the Baltic Sea drainage basin. *Meteor. Atmos. Phys.,* **77,** 61–73.

——, and Coauthors, 2001: A comprehensive model intercomparison study investigating the water budget during the Baltex-Pidcap period. *Meteor. Atmos. Phys.,* **77,** 19–44.

Jones, C. G., U. Willén, A. Ullerstig, and U. Hansson, 2004: The Rossby Centre regional atmospheric climate model. Part I: Model climatology and performance for the present climate over Europe. *Ambio,* **33** (4–5), 199–210.

Jones, R. G., J. M. Murphy, D. Hassell, and R. Taylor, 2001: Ensemble mean changes in a simulation of the European mean climate of 2071–2100 using the new Hadley Centre regional modelling system HadAM2H/HadRM3H. Hadley Centre Report, 19 pp.

Koster, R. D., M. J. Suarez, and M. Heiser, 2000: Variance and predictability of precipitation at seasonal-to-interannual timescales. *J. Hydrometeor.,* **1,** 26–46.

Kwadijk, J., 1993: The impact of climate change on the discharge of the river Rhine. Ph.D. thesis, Utrecht University, Netherlands, 201 pp.

Lenderink, G., B. van den Hurk, E. van Meijgaard, A. van Ulden, and H. Cuijpers, 2003: Simulation of present-day climate in RACMO2: First results and model developments. KNMI Tech. Rep. 252, 24 pp.

Ljungemyr, P., N. Gustafsson, and A. Omstedt, 1996: Parameterization of lake thermodynamics in a high resolution weather forecasting model. *Tellus,* **48A,** 608–621.

Masuda, K., Y. Hashimoto, H. Matsuyama, and T. Oki, 2001: Seasonal cycle of water storage in major river basins of the world. *Geophys. Res. Lett.,* **28,** 3215–3218.

Meier, H. E. M., R. Döscher, and T. Faxén, 2003: A multiprocessor coupled ice–ocean model for the Baltic Sea: Application to salt inflow. *J. Geophys. Res.,* **108,** 3273, doi:10.1029/2000JC000521.

Murphy, J., 2000: Predictions of climate change over Europe using statistical and dynamical downscaling techniques. *Int. J. Climatol.,* **20,** 489–501.

Nakicenovic, N., and R. Swart, Eds., 2000: *Special Report on Emission Scenarios*. Cambridge University Press, 570 pp.

Räisänen, J., and Coauthors, 2004: European climate in the late twenty-first century: Regional simulations with two driving global models and two forcing scenarios. *Climate Dyn.,* **22,** 13–31.

Roads, J. O., and Coauthors, 2003: GCIP water and energy budget synthesis (WEBS). *J. Geophys. Res.,* **108,** 8609, doi:10.1029/2002JD002583.

Sanchez, E., C. Gallardo, M. A. Gaertner, A. Arribas, and M. Castro, 2004: Future climate extreme events in the Mediterranean simulated by a regional climate model: First approach. *Global Planet. Change,* **44,** 163–180.

Schädler, C., 1985: Der Wasserhaushalt der Schweiz. Mitteilungen der Landeshydrologie No. 6, Bundesamt für Umweltschutz, Bern, Schweiz, Germany, 83 pp.

Schär, C., D. Luthi, U. Beyerle, and E. Heise, 1999: The soil-precipitation feedback: A process study with a regional climate model. *J. Climate,* **12,** 722–741.

——, P.-L. Vidale, D. Luethi, C. Frei, C. Haeberli, M. A. Liniger, and C. Appenzeiler, 2004: The role of increasing temperature variability in European summer heatwaves. *Nature,* **427,** 332–336.

Seneviratne, S. I., J. S. Pal, E. A. B. Eltahir, and C. Schär, 2002: Summer dryness in a warmer climate: A process study with a regional climate model. *Climate Dyn.,* **20,** 69–85.

——, P. Viterbo, D. Lüthi, and C. Schär, 2004: Inferring changes in terrestrial water storage using ERA-40 reanalysis data: The Mississippi River basin. *J. Climate,* **17,** 2039–2057.

Steppeler, J., G. Doms, U. Schättler, H. W. Bitzer, A. Gassmann, U. Damrath, and G. Gregoric, 2003: Meso-gamma scale forecasts using the non-hydrostatic model LM. *Meteor. Atmos. Phys.,* **82,** 75–96.

Takle, E. S., and Coauthors, 1999: Project to Intercompare Regional Climate Simulations (PIRCS): Description and initial results. *J. Geophys. Res.,* **104,** 19 443–19 461.

Trenberth, K. E., and C. J. Guillemot, 1995: Evaluation of the global atmospheric moisture budget as seen from analyses. *J. Climate,* **8,** 2255–2272.

van den Hurk, B. J. J. M., J. Ettema, and P. Viterbo, 2004: An analysis of the ECMWF soil analysis. KNMI Memo., 20 pp. [Available from KNMI, P.O. Box 201, 3730 AE De Bilt, Netherlands.]

Vidale, P.-L., D. Lüthi, C. Frei, S. Seneviratne, and C. Schär, 2003: Predictability and uncertainty in a regional climate model. *J. Geophys. Res.,* **108,** 4586, doi:10.1019/2002JD002810.

Viterbo, P., 1996: The representation of surface processes in general circulation models. Ph.D. thesis, ECMWF, Reading, United Kingdom, 201 pp.